Identification of $Cu_2(N_2)$ and $Cu_2(N_2)_2$ Complexes: Matrix Isolation and Density Functional Studies†

F. Elustondo and J. Mascetti*

Laboratoire de Physico-Chimie Moléculaire, Université Bordeaux I, 351, cours de la Libération, 33405 Talence Cedex, France

I. Pápai*

Institute of Isotope and Surface Chemistry, Spectroscopy Department, Chemical Research Centre of HAS, P.O.B. 77, H-1525 Budapest, Hungary

Received: October 13, 1999; In Final Form: January 20, 2000

Reactions of copper atoms with dinitrogen have been studied in argon and dinitrogen matrices at 10 K by UV−visible and FTIR spectroscopies. The co-condensation of copper vapor in neat dinitrogen matrices produces only the metal dimer 2:1 and 2:2 species, i.e., the $Cu_2(N_2)$ and $Cu_2(N_2)_2$ complexes. Density functional calculations carried out on these complexes indicate that N_2 coordinates to Cu_2 in end-on way. No reactivity occurs in argon dilute matrices when the dinitrogen−argon rate is lower than 50%. The reactivity of copper is greatly affected by the presence of CO in the matrix giving rise to mixed copper CO/N_2 species. The cooperative effect of CO is examined by DFT calculations. From both our experimental and theoretical results it is evident that only copper dimers exhibit a marked reactivity toward the N_2 molecule, whereas the naked Cu(0) atoms need the "help" of a reactive co-ligand like CO to promote the coordination of dinitrogen.

Introduction

Atoms and small clusters formed by thermal evaporation of metals under vacuum are much more reactive than those in their bulk form and are known to be able to form complexes with a large variety of molecules at low temperature. These reactions are of great interest both in catalysis and organometallic synthesis.[1,2] Furthermore, the study of dinitrogen fixation by metals is of particular importance for chemistry (activation and reduction of N_2),[3] biochemistry (mimetic reactions of nitrogenase),[4] and astrochemistry (models for nitrogen ices of interstellar grains).[5]

Thermally evaporated or laser ablated first row transition metal atoms (Ni,[6,7b] Co,[7] and Fe,[8] for instance) have been previously demonstrated to react with dinitrogen when trapped in cryogenic conditions. In most of these complexes, N_2 is coordinated to the metal in an end-on manner, but a few side-on species have been observed with Co[7a] and Fe.[8c,8d] Iron has also been proved to react both in its atomic and dimeric forms.[8d]

Previous studies related to the reactivity of matrix isolated copper atoms toward CO and NO in N_2 matrices have been reported by Cesaro and Dobos,[9,10] suggesting that nitrogen cannot be considered as a totally inert matrix medium. This prompted us to undertake the present experimental work, which represents a matrix isolation study of the reactivity of copper atoms and small copper clusters toward dinitrogen. Since a small amount of CO, produced during the vaporization of copper, was always present in our deposits, we have also investigated the influence of carbon monoxide on the reactivity of copper with nitrogen. To determine the equilibrium structure and the thermodynamical stability of the observed species, we have performed density functional calculations on conceivable reaction products.

This paper is organized as follows. In section 2, we describe the experimental conditions and computational methods we used. The experimental observations are presented in section 3.1. Both UV−visible and FTIR spectroscopies were used to characterize the systems we have studied: Cu/N_2, $Cu/N_2/Ar$, and $Cu/CO/N_2$, including isotopically labeled species ($^{15}N_2$). Section 3.2 gives the theoretical results obtained from density functional calculations. The experimental and theoretical findings are then discussed in section 4.

Experimental and Computational Details

The complete apparatus and the furnace used for metal vaporization have been previously described.[11,12] Atoms were generated by direct heating of a piece of copper pressed on a niobium ribbon, strung between two water-cooled copper electrodes. Copper (99.98%) and niobium were supplied by Goodfellow Metals. Ar (99.9995%) and N_2 (99.998%) were supplied by Air Liquide and were used without further purification. Isotopically substituted dinitrogen, $^{15}N_2$ (98% enriched), provided by Euriso-Top, was used to identify reaction products and to assign vibrational bands. The matrix molar ratio was always Cu/gas = 1/1000. The copper deposition rate was continuously controlled by using a quartz crystal microbalance. Copper and gases were co-condensed at 1 mmol/h for 2 to 4 h periods. Matrices were deposited on a CsBr window cooled to 10 K by means of a Cryophysics helium closed cycle cryogenerator Cryodine M22. Infrared spectra were recorded with a Bruker 113V interferometer at a resolution of 2 cm^{-1}. UV−visible spectra were made on the same samples using a PU8700 spectrometer with a resolution of 2 nm.

The density functional calculations were carried out using the B3LYP functional[13,14] as implemented in the *Gaussian 94*

† Part of the special issue "Marilyn Jacox Festschrift".

* Corresponding authors. E-mail: joelle@loriot.lsmc.u-bordeaux.fr; papai@iserv.iki.kfki.hu

10.1021/jp993663f CCC: $19.00
Published on Web 03/30/2000

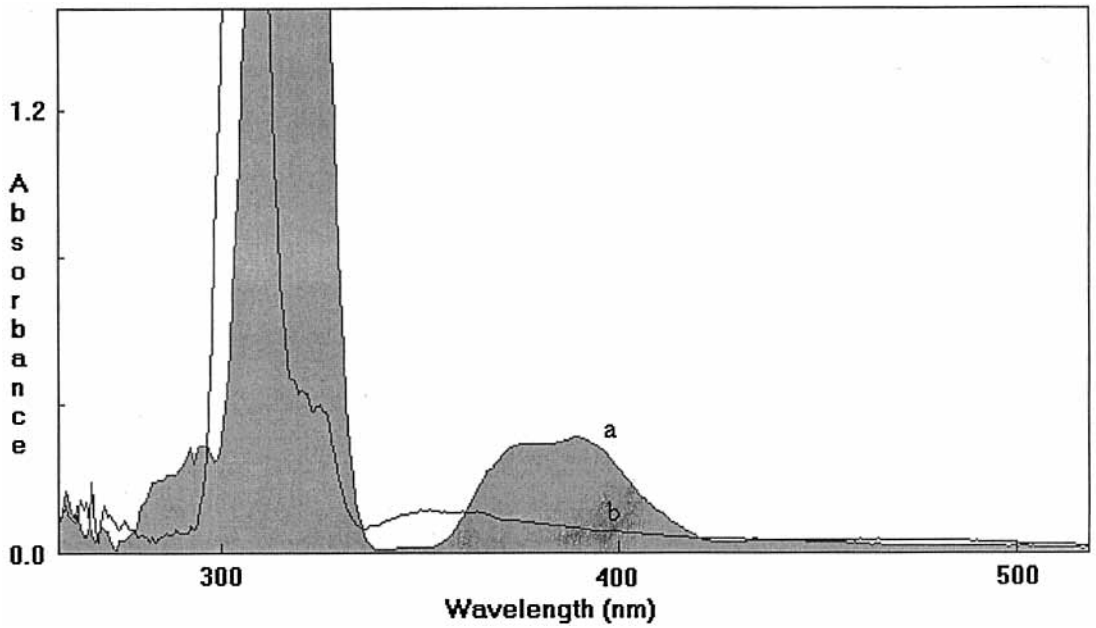

Figure 1. UV−visible spectra of (a) Cu/N_2 and (b) $Cu/N_2/Ar$ (N_2/Ar = 50%) deposits at 10 K.

package.[15] Schäfer's (14,9,5)/[8,5,3] all-electron basis set[16] supplemented with two polarization p functions[17] and a diffuse d function[18] was chosen for the Cu atom, while the 6-311G-(2d) basis set[15] was used for the light atoms. The geometries of the studied systems were fully optimized unless stated otherwise in the text. The harmonic vibrational frequencies were obtained from analytic energy second derivatives. The metal−ligand binding energies were calculated relative to the ground state fragments. For some of our investigated systems, we estimated the basis set superposition error (BSSE) contributions to the binding energies by using the counterpoise technique.[19] These contributions were calculated to be between 2 and 3 kcal/mol per metal−ligand bond. The reported binding energies refer to BSSE uncorrected values.

Results

3.1. Experimental Results. *3.1.1. Experiments in N_2 and N_2/Ar Matrices.* Electronic spectra of copper vapor condensed in various matrix media (except N_2) at 10 K have been presented by J. E. Hulse.[20] In argon, it was shown that copper atoms in their ground state ($3d^{10}\ 4s^1$) exhibit strong lines at 298, 302, and 306 nm. By annealing the matrix up to 30 K or by increasing the metal/argon ratio, transitions from copper clusters appear as thin bands between 230 and 280 nm and broad medium bands above 320 nm (Cu_2: 380 nm). Figure 1 shows our results obtained for neat and argon dilute nitrogen matrices. It is apparent that both Cu atoms and Cu_2 dimers are present in these matrices, and the presence of N_2 causes red shifts in the observed bands (the Cu main lines are at 307, 314, and 330 nm; the broad Cu_2 band is centered at 393 nm). Also, the Cu_2/Cu ratio becomes larger in neat nitrogen than in argon matrices (at the same temperature and metal/matrix ratio).

The FTIR spectrum (Figure 2) of copper vapor condensed at 10 K in neat nitrogen exhibits three bands at 2284 (m) and 2276 (sh), 2272 (ms) cm^{-1}. By annealing up to 26 K, the doublet at 2276, 2272 cm^{-1} grows and additional features at 2258, 2253 (sh), and 2239 cm^{-1} appear in the spectrum. When the deposit is made in argon dilute matrices (N_2/Ar = 50%), the band at 2284 cm^{-1} becomes the most intense in the spectrum; annealing up to 30 K induces the growth of bands at 2272 (m), 2254 (m), and 2235 (w) cm^{-1}. When the nitrogen/argon ratio is lowered to 10%, no bands are observed in the 2300−2200 cm^{-1} region and only weak features assigned to copper carbonyl species are observed (Cu(CO) at 2010 (m) cm^{-1}; $Cu(CO)_3$ at 1984, 1977 (vw) cm^{-1}; $Cu(CO)_2$ at 1890 (w) cm^{-1}),[21,22] along with weak bands located at 1933 and 1918 cm^{-1}. These latter bands have recently been observed by Cesaro and Dobos[9,10] as well and they were tentatively assigned to mixed $Cu/N_2/CO$ species. The annealing and concentration effects suggest that three different copper/nitrogen species are formed: the band at 2284 cm^{-1} belongs to the lowest N_2 stoichiometry species, whereas the bands at 2258 and 2253 cm^{-1} are due to a compound of higher nitrogen stoichiometry.

Isotopic effects were measured in neat $^{15}N_2$ matrices showing that the bands at 2284, 2276, and 2272 cm^{-1} are shifted to 2208, 2199, and 2197 cm^{-1}, respectively. The doublet at 2258/2253 cm^{-1}, which grows by annealing above 26 K is shifted to 2182/2177 cm^{-1}. Experiments done with mixtures of $^{14}N_2/^{15}N_2$ showed that no intermediate values occurred between the absorptions of $^{14}N_2$ and $^{15}N_2$ compounds. This implies that the observed copper/nitrogen complexes are either monoligand species, or they contain more than one nitrogen, but no vibrational coupling exists between the NN stretching vibrations. The latter case can occur if the N_2 molecules are attached to different metallic centers of Cu_n ($n > 1$).

3.1.2. Experimental Results in CO-Doped N_2 Matrices. As noted before, due to carbon impurities of the copper ribbon, a small amount of CO was always present in the deposits. Depending on the piece of metal we used, the quantity of CO slightly varied in our experiments. Keeping all deposit parameters identical (metal flow rate = 1 mmol/h, time of deposit = 4h), we have been able to observe the influence of the presence of CO on the reactivity of copper atoms. Our results obtained for deposits with increasing amount of CO are summarized in Table 1, together with the results previously reported by Cesaro and Dobos[9,10] on co-condensation of Cu and CO in N_2 matrices.

It appears from Table 1 that the formation of $Cu_n(N_2)_m$ complexes is not affected by the presence of a small amount of CO. As the rate of CO deposition increases, the formation of mixed N_2/CO and pure carbonyl complexes is favored and the intensity of the bands at 2272 and 2258/2253 cm^{-1}, associated with pure copper−nitrogen complexes, decrease. Finally, when

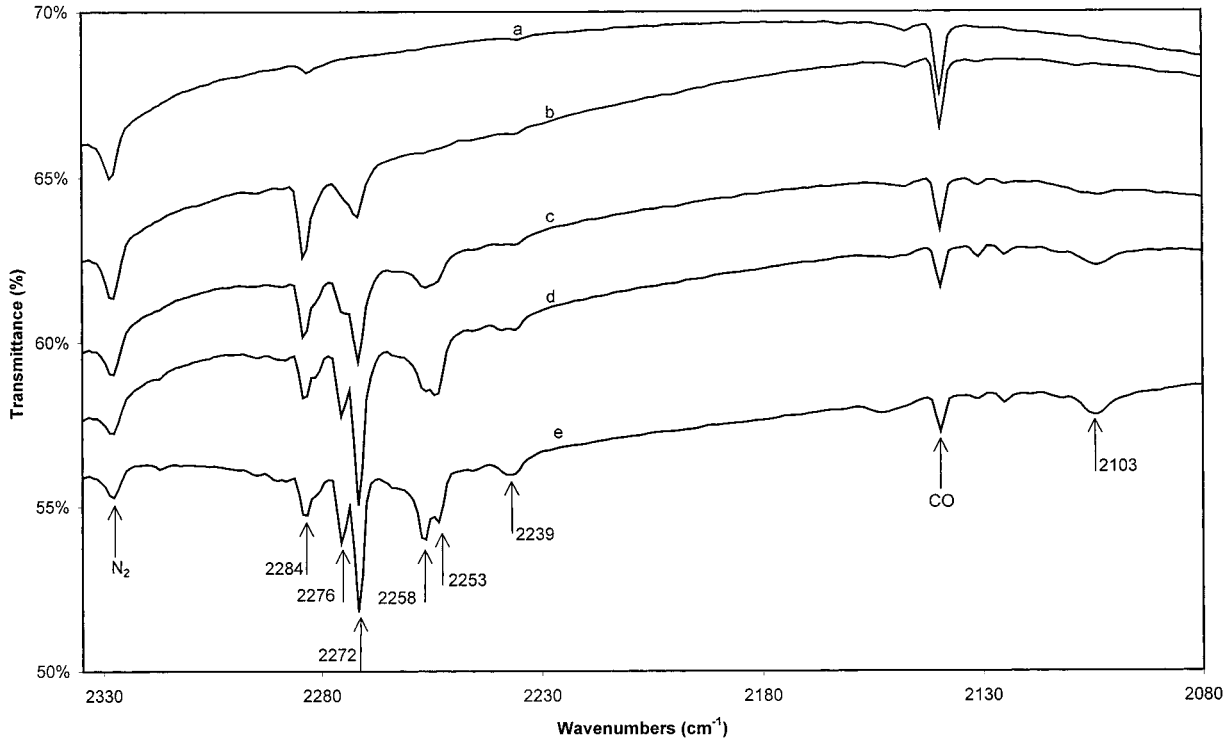

Figure 2. FTIR spectra of Cu/N_2 deposits: (a) neat N_2, (b) Cu/N_2 at 10 K, and (c), (d), (e) after annealing up to 22, 26, and 30 K, respectively.

TABLE 1: Observed ν(NN) and ν(CO) Frequencies (in cm^{-1}) of Cu Complexes Formed in N_2 Matrices[a]

low CO rate[b]	medium CO rate[b]	high CO rate[b]	from ref 9, 10.	assignments
2284 (m)	2283 (s)			$Cu_n(N_2)_m$
2276 (m)				$Cu_n(N_2)_m$
2272 (s)	2272 (w)			$Cu_n(N_2)_m$
2257 (m), 2255 (m)	2253 (vw)			$Cu_n(N_2)_m$
	2245 (vw)			$Cu_n(N_2)_m$
2239 (w), 2236 (w)				$Cu_n(N_2)_m$
		2200 (vw)	2199 ν(NN)	$Cu_n(CO)_m(N_2)_{m'}$
	2132 (vw)	2132 (w)		$Cu_n(CO)_m(N_2)_{m'}$
	2120 (w)	2120 (w)	2117 ν(NN)	$Cu_n(CO)_m(N_2)_{m'}$
		2113 (w)	2111 ν(NN)	$Cu_n(CO)_m(N_2)_{m'}$
2103 (w)	2104 (vw)	2102 (m)		$Cu_3(CO)$
		2039 (w)	2039 ν(CO)	$Cu_n(CO)_m(N_2)_{m'}$
		2031 (w)	2029 ν(CO)	Cu(CO)
		1986 (m)		$Cu(CO)_3$
		1975 (w)		$Cu(CO)_3$
1917 (vw)	1917 (m)	1917 (m)	1919 ν(CO)	$Cu_n(CO)_m(N_2)_{m'}$
	1911 (w)	1913 (w)		$Cu_n(CO)_m(N_2)_{m'}$
1907 (w)	1907 (m)	1906 (s)	1906 ν(CO)	$Cu_n(CO)_m(N_2)_{m'}$

[a] IR intensities are indicated in parentheses (s = strong, m = medium, w = weak, vw = very weak). [b] Present work. Low, medium, and high CO rates refer to $A_{\nu(CO)} < 0.05$, $0.05 < A_{\nu(CO)} < 0.2$, and $A_{\nu(CO)} > 0.2$, respectively, where $A_{\nu(CO)}$ is the absorbance of the free CO band at 2140 cm^{-1}.

the absorption of the ν(CO) mode at 2140 cm^{-1} is greater than 0.2, no more pure N_2 complexes are detected, and polymetallic carbonyls are formed ($Cu_3(CO)$ at 2102 cm^{-1}). The ν(NN) and ν(CO) modes of mixed $Cu(N_2)_n(CO)_m$ species are located between 2150 and 1900 cm^{-1} and are the most intense features of the spectrum. Our results show evidence for the formation of these mixed N_2/CO complexes through the small isotopic shift obtained for the ν(CO) modes by isotopic labeling with $^{15}N_2$. For example, ν(CO) bands at 1917 and 1906 cm^{-1} of mixed N_2/CO copper complexes are respectively shifted by 5 and 10 cm^{-1} in $^{15}N_2$ matrices.

3.2. Theoretical Results. *3.2.1. $Cu(N_2)_n$ Complexes.* First we examined the interaction of a Cu atom with a single N_2 molecule. We derived potential energy curves for the three possible N_2 coordination modes, i.e., the linear end-on (α(CuNN) = 180.0°), bent end-on (α(CuNN) = 140.0°), and side-on arrangements (α(CuXN) = 90.0°, where X is the midpoint of N_2). In these calculations, the NN bond length (R(NN)) was fixed at its calculated equilibrium value, and the R(CuN) distance was varied for each case. The results are shown in Figure 3, where for comparison we also depicted the curve obtained for the bent end-on Cu(CO) molecule. This latter complex was shown to have a bent equilibrium geometry[23−29] and to be bound by about 10 kcal/mol at a level of theory[27] similar to what is applied here.[30] Unlike Cu(CO), the $Cu(N_2)$ molecule is predicted to be unstable with respect to the dissociation limit, as indicated by the repulsive nature of the $Cu-N_2$ curves. The $Cu(N_2)$ molecule is still unstable, even for the bent arrangement, when the geometry constraints are released. Although the geometry optimization finds a very shallow minimum at R(CuN) = 2.3 Å, R(NN) = 1.098 Å, and α(CuNN) = 132.9°, the interaction energy is practically zero.

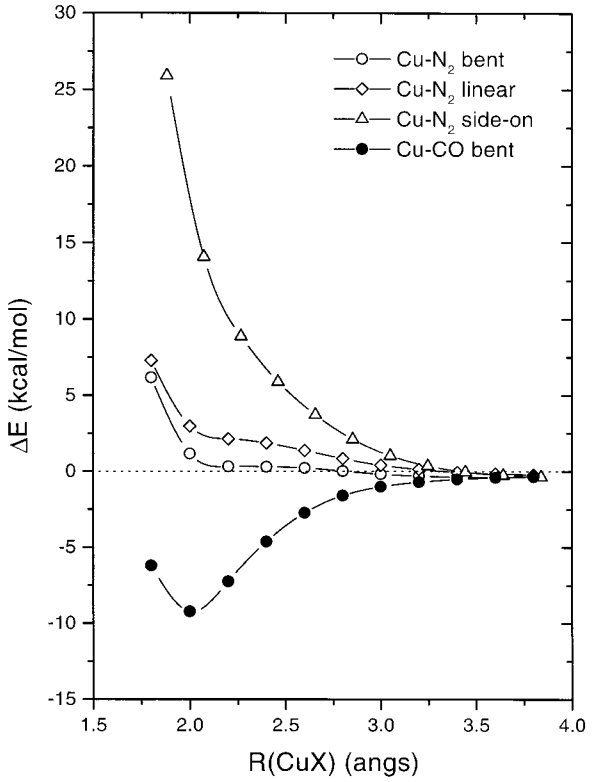

Figure 3. Interaction of Cu with N_2 and CO in various geometrical arrangements as a function of R(CuN) (R(NN) = 1.091 Å, R(CO) = 1.125 Å; α(CuNN) = α(CuCO) = 140.0° (for the bent end-on geometry)).

TABLE 2: Optimized Geometries and Binding Energies of $Cu(N_2)_n$ (n = 1, 2, 3) Complexes[a]

	$n=1$	$n=2$	$n=3$
symmetry (state)	C_s (^{2}A′)	C_{2v} (^{2}A$_1$)	D_{3h} (^{2}A$_2$″)
R(CuN)	2.297	1.916	1.907
R(NN)	1.098	1.114	1.110
α(CuNN)	132.9	154.8	180.0
α(NCuN)		158.6	120.0
D_e	−0.1	−1.0	4.7

[a] Bond lengths (R) and angles (α) are given in Å and degrees, binding energies (D_e) in kcal/mol (with respect to Cu + nN$_2$). The calculated R_e for free N_2 is 1.091 Å.

We then optimized the structures of the $Cu(N_2)_2$ and $Cu(N_2)_3$ complexes. The results for the entire $Cu(N_2)_n$ (n = 1, 2, 3) series are given in Table 2. For $Cu(N_2)_2$, an energy minimum is found for a flat "w" shape C_{2v} structure, but in fact, it is above Cu + 2N_2 in energy. The $Cu(N_2)_3$ molecule has a D_{3h} structure and it is the only member in this series with appreciable binding energy (4.7 kcal/mol). Considering that the BSSE at the present level of theory amounts to 2−3 kcal/mol per metal−ligand bond, the formation of this complex is very unlikely too, not only due to the small binding energy, but also because its $Cu(N_2)$ and $Cu(N_2)_2$ precursors are unstable. Moreover, the calculated frequency of the IR active NN stretching mode (e′) of $Cu(N_2)_3$ is 2114 cm^{-1}, which is far from any observed NN stretching bands.

3.2.2. $Cu_2(N_2)_n$ Complexes. The coordination modes of N_2 to Cu_2 considered in our study are shown in Figure 4. The corresponding interaction energy curves are plotted in Figure 5. The calculations reveal that the bridge forms of $Cu_2(N_2)$ are not favored at all and of the two atop forms, only the end-on mode (A_I in Figure 5) is predicted to be bound with respect to Cu_2+N_2. The binding energy after the geometry optimization

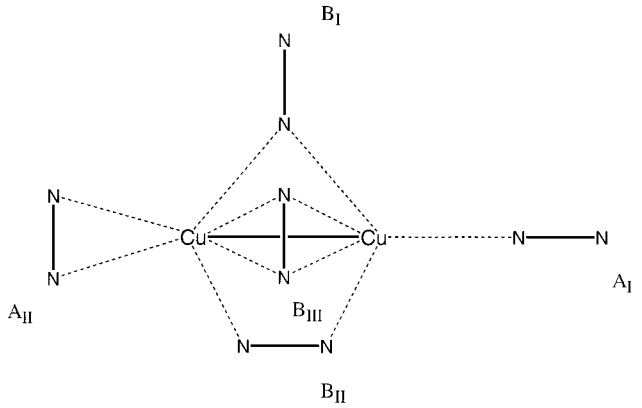

Figure 4. Various geometrical arrangements for the Cu_2+N_2 interaction. A_I and A_{II} are two "atop" Cu_2-N_2 forms, while B_I, B_{II}, and B_{III} correspond to "bridge" coordinations.

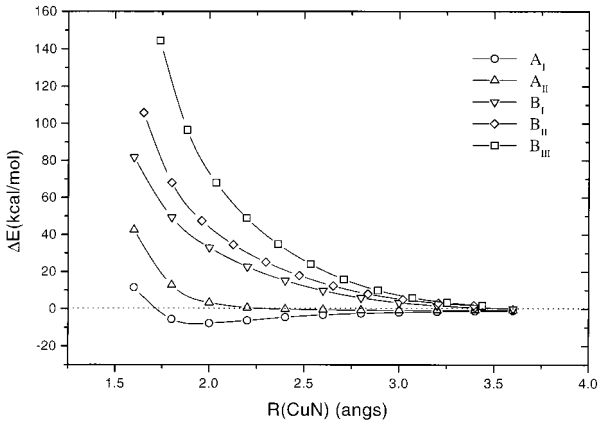

Figure 5. Interaction of Cu_2 with N_2 for different coordination modes (R(CuCu) = 2.264 Å, R(NN) = 1.091 Å).

TABLE 3: Calculated Properties of $Cu_2(N_2)_n$ (n = 1, 2) Complexes[a]

	$n=1$	$n=2$
symmetry (state)	$C_{\infty v}$ ($^1\Sigma_g$)	C_2 (^{1}A)
R(CuCu)	2.267	2.281
R(CuN)	1.960	2.000
R(NN)	1.095	1.096
α(CuNN)	180.0	167.2
α(CuCuN)	180.0	174.4
D_e	7.9	12.8
ω(NN str)	2378 (105)[b]	sym: 2372 (2), asym: 2367 (260)[c]
ω(CuCu str)[d]	299 (0.6)	288 (0)
ω(CuN str)[d]	204 (1.1)	asym: 209 (0.2), sym: 170 (0.3)[c]

[a] Bond lengths (R) and angles (α) are given in Å and degrees, binding energies (D_e) in kcal/mol (with respect to Cu_2 + nN$_2$), harmonic vibrational frequencies (ω) in cm^{-1}. The calculated equilibrium parameters for the free Cu_2 and N_2 fragments are $R_e(Cu_2)$ = 2.264 Å, $\omega_e(Cu_2)$ = 253 cm^{-1}, $R_e(N_2)$ = 1.091 Å, $\omega_e(N_2)$ = 2438 cm^{-1}. [b] Intensities are given in parentheses. [c] "sym" and "asym" refer to A and B symmetry motions, respectively. [d] The CuCu str and CuN str vibrations are coupled in both complexes.

is 7.9 kcal/mol (see Table 3). The $Cu_2(N_2)$ complex is linear, but it can easily bend, as indicated by the flat bending potential (ω(CuCuN bend) = 34 cm^{-1}). The nitrogen is only weakly bound in this complex, and therefore both Cu_2 and N_2 fragments are only slightly elongated upon coordination. The NN stretch frequency in $Cu_2(N_2)$ is shifted down by 60 cm^{-1} from that of the free N_2.

Our calculations show that the copper dimer can bind a second N_2 at the other atop position. The nitrogen ligands in $Cu_2(N_2)_2$ are bound by 12.8 kcal/mol, which means that the binding

TABLE 4: Calculated Properties of $Cu_3(N_2)$[a]

	$Cu_3(N_2)$ ($^2B_2$)	Cu_3 ($^2B_2$)
$R(Cu^bCu^b)$	2.453	2.633
$R(Cu^aCu^b)$	2.349	2.324
$R(Cu^aN)$	1.911	
R(NN)	1.100	
D_e	13.6	
ω(NN str)	2262 (1351)	
ω(CuN str)	338 (6)	
ω(CuCu str)	218 (6), 164 (2)	245 (1), 157 (15)

[a] For units, see Table 3. Cu^a and Cu^b denote the *apex* and *base* atoms of Cu_3.

energy of the second N_2 is 4.9 kcal/mol. The energy minimum of $Cu_2(N_2)_2$ corresponds to a C_2 structure, where the two N_2 ligands coordinate to Cu_2 in an almost linear arrangement (α-(CuNN) = 167°, α(CuCuN) = 174°). The CuCu and CuN bonds in $Cu_2(N_2)_2$ are slightly longer than in $Cu_2(N_2)$, but the NN bond lengths are very similar in the 2:1 and 2:2 complexes. The two NN stretch frequencies split up by only 5 cm^{-1}, and the asymmetric combination is predicted to lie lower in frequency and to be far more intense in IR than the symmetric NN stretch. The calculated shifts of these two bands from that of the free N_2 molecule are 66 and 71 cm^{-1}.

We have also computed the $^{14}N_2/^{15}N_2$ isotopic frequency shifts for the NN stretching vibrations of both $Cu_2(N_2)$ and $Cu_2(N_2)_2$ molecules. The calculated red shifts are 79 cm^{-1} for $Cu_2(N_2)$ and 81/80 cm^{-1} for the symmetric/asymmetric NN stretching modes of $Cu_2(N_2)_2$.

3.2.3. The $Cu_3(N_2)$ Complex. The coordination of a single N_2 molecule with the ground state ($^2B_2$) of Cu_3 (see ref 32 and references therein) yields a planar C_{2v} structure, in which N_2 is end-on coordinated to the apex Cu atom of the Jahn−Teller distorted copper triangle. Similarly to what was found for $Cu_3(CO)$,[33] the binding of N_2 reduces the Jahn−Teller distortion and brings the Cu_3 triangle closer to equilateral structure (see Table 4).

The N_2 molecule forms a stronger bond with Cu_3 than with Cu_2: its binding energy in the $Cu_3(N_2)$ complex is 13.6 kcal/mol. In line with this, the CuN stretch frequency (338 cm^{-1}) and the shift of the NN stretch absorption (156 cm^{-1}) are calculated to be notably larger for $Cu_3(N_2)$ than the corresponding values for $Cu_2(N_2)$. Our calculations predict the NN stretch band to be very intense in IR.

3.2.4. Mixed CO/N_2 Complexes. To investigate the effect of the CO co-ligand on the N_2 coordination and to see the stability of possible mixed carbonyl−dinitrogen species, we carried out calculations for the $Cu(CO)(N_2)$, $Cu(CO)(N_2)_2$, and $Cu(CO)_2(N_2)$ mixed complexes. Our results are summarized in Table 5.

Note first that, unlike for $Cu(N_2)$, the N_2 molecule is clearly bound in $Cu(CO)(N_2)$. The calculated N_2 binding energy in this complex is 7.5 kcal/mol and the Cu−N bond length is 1.84 Å. The Cu−CO interaction becomes stronger as well when going from the 1:1 to the mixed $Cu(CO)(N_2)$ system. While the CO binding energy in Cu(CO) is 9.5 kcal/mol, it is predicted to be notably larger (17.2 kcal/mol) in $Cu(CO)(N_2)$. These results suggest that the binding in the mixed $Cu(CO)(N_2)$ complex is strongly cooperative, i.e., the energy to break both metal−ligand bonds is much larger than the sum of binding energies in the separate monoligand complexes. Not only does the CO binding energy change upon N_2 coordination, but also does its coordination mode. As pointed out in several previous theoretical works,[23−29] the Cu(CO) complex has a bent equilibrium structure. Our calculations show that the CuCO unit becomes linear when N_2 is attached to it. The CuNN part of $Cu(CO)(N_2)$ is linear as well, and actually the energy minimum of the mixed $Cu(CO)(N_2)$ corresponds to a linear equilibrium geometry. The strengthening of the Cu−L bonds in $Cu(CO)(N_2)$ is also apparent from the calculated vibrational frequencies. The CO stretching frequency in Cu(CO) is shifted down by 163 cm^{-1} relative to that in free CO, whereas this shift is 207 cm^{-1} in $Cu(CO)(N_2)$. The stretching frequency of the N_2 molecule shifts down by 273 cm^{-1} upon coordination to Cu(CO). As noted in Table 5, the CO str and NN str vibrations are strongly coupled in $Cu(CO)(N_2)$.

TABLE 5: Calculated Properties of $Cu(CO)(N_2)$, $Cu(CO)(N_2)_2$, and $Cu(CO)_2(N_2)$ along with Those of Cu(CO) and CuN_2[a]

	$Cu(CO)(N_2)$	$Cu(CO)(N_2)_2$	$Cu(CO)_2(N_2)$	Cu(CO)	CuN_2
R(CuC)	1.825	1.849	1.870	1.969	
R(CO)	1.149	1.144	1.142	1.140	
R(CuN)	1.835	1.943	1.985		2.297
R(NN)	1.117	1.106	1.102		1.098
α(CuCO)	180.0	180.0	179.2	139.7	
α(CuNN)	180.0	179.2	180.0		132.9
α(CCuN)	180.0	127.1	113.5		
D_e(Cu−CO)[b]	17.2		20.6	9.5	
D_e(Cu−N_2)[b]	7.5	4.8			−0.1
ω(CO str)	2010[c]	2044[c]	2093 (sym)[c] 2038 (asym)	2054	
ω(NN str)	2165[c]	2267 (sym)[c] 2156 (asym)	2265[c]		2326

[a] For units, see Table 3. The calculated equilibrium parameters for the free CO and N_2 are $R_e(CO)$ = 1.125 Å, $\omega_e(CO)$ = 2217 cm^{-1}, $R_e(N_2)$ = 1.091 Å, $\omega_e(N_2)$ = 2438 cm^{-1}. [b] D_e(Cu−CO) and D_e(Cu−N_2) denote CO and N_2 binding energies in kcal/mol (for mixed species, they are equal to the energies of the $Cu(CO)_n(N_2)_m \rightarrow Cu(CO)_{n-1}(N_2)_m$ + CO and $Cu(CO)_n(N_2)_m \rightarrow Cu(CO)_n(N_2)_{m-1}$ + N_2 reactions). [c] In these modes, the CO str and NN str motions are strongly coupled.

The $Cu(CO)(N_2)$ complex is able to bind another N_2 or a CO molecule resulting in the $Cu(CO)(N_2)_2$ and $Cu(CO)_2(N_2)$ molecules. The binding energy of the second N_2 in $Cu(CO)(N_2)_2$ is 4.8 kcal/mol, while the second CO in $Cu(CO)_2(N_2)$ is bound by 20.6 kcal/mol (see Table 5). Both $Cu(CO)(N_2)_2$ and $Cu(CO)_2(N_2)$ complexes have planar (C_{2v}) equilibrium structures with linear CuCO and CuNN units. The Cu−C and Cu−N bonds in these complexes are elongated with respect to those in the $Cu(CO)(N_2)$ molecule. Consequently, the frequency shifts for the CO str and NN str modes are always smaller in the $Cu(CO)(N_2)_2$ and $Cu(CO)_2(N_2)$ complexes than in $Cu(CO)(N_2)$. Similarly to $Cu(CO)(N_2)$, these modes are not pure CO stretching and NN stretching vibrations. In $Cu(CO)(N_2)_2$, the symmetric combination of the NN str vibrations couples with CO str, while a similar coupling between the symmetric combination of the two CO str vibrations and the NN str exists in the $Cu(CO)_2(N_2)$ complex.

4. Discussion

Results obtained by UV−visible spectroscopy show that, as previously observed for nickel[6d] and iron,[8d,8e] the formation of metal aggregates depends on the dinitrogen concentration of the matrix: at 10 K, for the same metal/matrix molar ratio (1/1000) during deposition, the Cu_2/Cu ratio in the matrix is higher in neat nitrogen matrices than in argon and decreases when dilution in argon increases. One possible explanation for this phenomenon is that the diffusion of the Cu atoms is enhanced due to the microheterogeneous structure of binary N_2/Ar solid mixtures, as described by Becker et al.[34]

Because of the similarity of their electronic structure, the coordination of CO and N_2 molecules to transition metal atoms generally gives rise to analogue binary complexes.[35] This, however, does not seem to be valid for copper. Although the existence of both the $Cu(CO)_n$ ($n = 1, 2, 3$) and $Cu_n(CO)$ ($n =$ 1 to 4) series has been clearly demonstrated,[21] our experimental and theoretical results show that Cu atoms are inactive toward N_2. If the $Cu(N_2)_n$ complexes exist, they are probably very weakly bound van der Waals complexes with binding energies similar to those of $Al(N_2)_n$ complexes.[36]

Contrary to atomic Cu, Cu_2 forms stable albeit weak complexes with N_2. Our experimental findings (the presence of Cu_2 lines in the electronic spectra; the annealing effects; the absence of vibrational coupling between nitrogens) suggest the following assigment for the three species observed in neat N_2 matrices: $Cu_2(N_2)$, $\nu(NN) = 2284$ cm^{-1}; $Cu_2(N_2)_2$, $\nu(NN) =$ 2276/2272 cm^{-1}; $Cu_n(N_2)_m$ with $n > 2$ and $m > 2$, $\nu(NN) =$ 2258, 2253, and 2239 cm^{-1}. The assignment for the first two species is supported by the results of our DFT calculations since (1) the predicted shifts in the ν(NN) frequencies with respect to that of free N_2 (60 cm^{-1} for $Cu_2(N_2)$ and 66/71 cm^{-1} for $Cu_2(N_2)_2$) match reasonably well with the observed shifts (48 cm^{-1} for $Cu_2(N_2)$ and 56/60 cm^{-1} for $Cu_2(N_2)_2$); (2) the calculated $^{14}N_2/^{15}N_2$ isotopic shifts of the ν(NN) modes (79 cm^{-1} for $Cu_2(N_2)$ and 80 cm^{-1} for $Cu_2(N_2)_2$) are in line with the experimental shifts (76 cm^{-1} for $Cu_2(N_2)$ and 77 cm^{-1} for $Cu_2(N_2)_2$).

The 2276/2272 cm^{-1} doublet could be assigned to the in-phase (sym) and out-of-phase (asym) NN stretching vibrations of the $Cu_2(N_2)_2$ complex, but the predicted IR intensities (2 and 260 km/mol, see Table 3) suggest that only the out-of-phase vibration should be observed in the IR spectra. Moreover, the predicted isotope effects for the $Cu_2(^{14}N_2)(^{15}N_2)$ species indicate that additional components between the $Cu_2(^{14}N_2)_2$ and $Cu_2(^{15}N_2)_2$ bands should appear in the spectra, which were not observed in our measurements. Therefore, the 2276/2272 cm^{-1} doublet splitting is probably due to site effect of the N_2 matrix.

More precise stoichiometry for the other $Cu_n(N_2)_m$ species cannot be given from our present experimental and theoretical evidences. It is likely, however, that the $Cu_3(N_2)$ molecule is not present among the produced species. From our calculations ($\Delta\omega(NN) = 156$ cm^{-1}), a strong absorption around 2180 cm^{-1} should be observed, which is absent in our IR spectra (see Figure 2).

The CO and N_2 molecules are isoelectronic and their coordination to metal atoms is generally described in terms of the donation/back-donation model. Because the π^* orbital of CO is localized on C atom, while the corresponding N_2 orbital is delocalized, the back-donation is larger in carbonyl complexes, and the metal−CO interaction is always stronger than in the metal−N_2 interaction in analogue systems.[37] Another characteristic aspect of the metal−CO and metal−N_2 bonds is the σ repulsion between the ligand lone pairs and the filled or partially filled metal orbitals, which is usually reduced through metal s−d hybridization. This repulsion is quite enhanced for the closed shell ($4s^1\,3d^{10}$) Cu atom, and the Cu−CO bond is already a relatively weak bond as compared to those in "true" transition metal complexes.[31] It is therefore not surprising to find no reactivity between Cu atoms and N_2. As pointed out by Fournier,[33] the σ repulsion is reduced in Cu_2−L complexes because the 4s derived Cu_2 orbitals can more easily polarize away from the ligand than the 4s orbital of the Cu atom. For this reason, the $Cu_2(N_2)$ complex is already bound, but only in the A_1 arrangement (see Figure 4). Similar results have been previously obtained for the Cu/C_2H_4 system[38] in that the $Cu_2(C_2H_4)_2$ complex was more easily formed than the 1:1 complex.

The σ repulsion between the Cu atom and N_2 can also be reduced by attaching co-ligands to metal (CO in our case) prior to N_2 coordination. The co-ligand induced hybridization of the metal orbitals allows more favorable interaction with the π^* N_2 orbitals, leading to the formation of mixed CO/N_2 species. Similar cooperative effects have been observed in our previous study on the Ni/CO_2 system, where the coordination of CO_2 was promoted by using N_2 enriched matrices.[39]

Although the identification of the produced $Cu_n(CO)_m(N_2)_{m'}$ complexes was out of the scope of the present study, useful observations may emerge from a comparison of the IR spectra of our $Cu/CO/N_2$ deposits (Table 1) with the predicted CO str and NN str frequencies of the $Cu(CO)(N_2)$, $Cu(CO)(N_2)_2$, and $Cu(CO)_2(N_2)$ complexes (Table 5). The CO str absorptions of the observed $Cu_n(CO)_m(N_2)_{m'}$ species are shifted down from the free CO band (2140 cm^{-1}) by $\Delta\omega(CO)\sim$220−230 cm^{-1}. Such a large $\Delta\omega$(CO) is calculated only for the $Cu(CO)(N_2)$ complex (207 cm^{-1}). The predicted $\Delta\omega$(NN) for this molecule is 273 cm^{-1}, which is much larger than the observed shifts (130−220 cm^{-1}). For the $Cu(CO)(N_2)_2$ and $Cu(CO)_2(N_2)$ complexes, the calculated $\Delta\omega$(CO) values (173 cm^{-1} for $Cu(CO)(N_2)_2$ and 124 and 179 cm^{-1} for $Cu(CO)_2(N_2)$) are too small. All of these data suggest that none of the observed $Cu_n(CO)_m(N_2)_{m'}$ species are identical to the $Cu(CO)(N_2)$, $Cu(CO)(N_2)_2$, and $Cu(CO)_2(N_2)$ complexes. We note that Cesaro and Dobos arrived at the same conclusion in their studies.[9,10] Clearly, more work is required from both experimental and theoretical sides to be able to identify the observed mixed species.

5. Conclusion

We have shown in this paper that dinitrogen binds more likely to copper clusters than to copper atoms and the formation of two end-on species is proposed from our experimental and theoretical studies: the $Cu_2(N_2)$ and $Cu_2(N_2)_2$ complexes. The metal−ligand interaction in these complexes is rather weak, as judged from the predicted binding energies. Further Raman experiments are in progress in our laboratory to characterize the Cu−Cu and Cu−N stretching vibrational modes in these species.

To allow N_2 coordination to atomic copper, one must take advantage of the cooperative effects of CO ligands. The presence of a small amount of CO in the matrix leads to the formation of mixed monometallic complexes, for which the ligand binding energies are significantly larger than those of the independent binary moieties.

Finally, we point out that the role played by dinitrogen in the formation of metal aggregates in low-temperature matrices and its ability to bind to transition metal atoms and/or aggregates should be kept in mind when using N_2 as an "inert" matrix material.

Acknowledgment. J.M. and I.P. acknowledge financial support from CNRS and the Hungarian Academy of Sciences. This work was also partially supported by grants OTKA (T029926) and AKP (97-102 2, 4/32).

References and Notes

(1) *Chemistry and Physics of Matrix Isolated Species*; Andrews, L., Moskovits, M., Eds.; North-Holland: Amsterdam, 1989.

(2) (a) Burdett, J. K. *Coord. Chem. Rev.* **1978**, *27*, 1. (b) Almond, M. J. *Chem. Soc. Rev.* **1994**, *23*, 309.

(3) Billiau, F. *Actualité Chimique* **1982**, *1*, 9.

(4) Schwarz, J. *J. Phys. Chem.* **1995**, *99*, 11405.

(5) (a) McKinnon, W. B. *Nature* **1995**, *375*, 535. (b) Ehrenfreund, P. *Icarus* **1997**, *130*, 1.

(6) (a) Burdett, J. K.; Turner, J. J. *Chem. Comm*. **1971**, 885. (b) Huber, H. H.; Kundig, E. P.; Moskovits, M.; Ozin, G. A. *J. Am. Chem. Soc*. **1973**, *95*, 332. (c) Klotzbucher, W.; Ozin, G. A. *J. Am. Chem. Soc*. **1975**, *97*, 2672. (d) Galan, F. Thesis, Université Bordeaux I, 1994. (e) Manceron, L.; Alikhani, M. E.; Joly, H. A. *Chem. Phys*. **1998**, *228*, 73.

(7) (a) Ozin, G. A.; Van der Voet, A. *Can. J. Chem*. **1973**, *51*, 637. (b) Andrews, L.; Citra, A.; Chertihin, G. V.; Bare, W. D.; Neurock, M. *J. Phys. Chem*. **1998**, *102*, 2561.

(8) (a) Doeff, M. M.; Parker, S. F.; Barrett, P. H.; Pearson, R. G. *Inorg. Chem*. **1984**, *23*, 4108. (b) Barett, P. H.; Montano, P. A. *J. Chem. Soc., Faraday Trans. 2* **1978**, *73*, 379. (c) Chertihin, G. V.; Andrews, L.; Neurock, M. *J. Phys. Chem*. **1996**, *100*, 14609. (d) Elustondo, F. Thesis, Université Bordeaux I, 1998. (e) Elustondo, F.; Mascetti, J.; Papai, I., to be published.

(9) Cesaro, S. N.; Dobos, S. *Mikrokim. Acta (Suppl.)* **1997**, *14*, 387.

(10) Dobos, S.; Cesaro, S. N. *High Temp. Mater. Sci*. **1997**, *37*, 81.

(11) (a) Cosse-Mertens, C. Thesis, Université Bordeaux I, 1981. (b) Elustondo, F. Thesis, Université Bordeaux I, 1998.

(12) Tranquille, M. *Spectra 2000* **1984**, *98*, 43.

(13) Becke, A. D. *J. Chem. Phys*. **1993**, *98*, 5648.

(14) Lee, C.; Yang, W.; Parr, R. G. *Phys. Rev. B* **1988**, *37*, 785.

(15) Frisch, M. J.; Trucks, G. W.; Schlegel, H. B.; Gill, P. M. W.; Johnson, B. G.; Robb, M. A.; Cheeseman, J. R.; Keith, T.; Petersson, A.; Montgomery, J. A.; Raghavachari, K.; Al-Laham, M. A.; Zakrzewski, V. G.; Ortiz, J. V.; Foresman, J. B.; Peng, C. Y.; Ayala, P. Y.; Chen, W.; Wong, M. W.; Andres, J. L.; Replogle, E. S.; Gomperts, R.; Martin, R. L.; Fox, D. J.; Binkley, J. S.; Defrees, D. J.; Baker, J.; Stewart, J. P.; Head-Gordon, M.; Gonzalez, C.; Pople, J. A. *Gaussian 94*; Gaussian, Inc.: Pittsburgh, PA, 1995.

(16) Schäfer, A.; Horn, H.; Ahlrichs, R. J. *Chem. Phys*. **1992**, *97*, 2571.

(17) Wachters, A. J. H. *J. Chem. Phys*. **1970**, *52*, 1033.

(18) Hay, P. J. *J. Phys. Chem*. **1977**, *66*, 43.

(19) Boys, S. B.; Bernardi, F. *Mol. Phys*. **1970**, *19*, 553.

(20) Hulse, J. E. Thesis, University of Toronto, 1978.

(21) (a) Moskovits, M.; Hulse, J. E. *J. Phys. Chem*. **1977**, *81*, 2004. (b) Chenier, J. H. B.; Hampson, C. A.; Howard, J. A.; Mile, B. *J. Phys. Chem*. **1989**, *93*, 114. (c) Kasai, P. H.; Jones, P. M. *J. Am. Chem. Soc*. **1985**, *107*, 813.

(22) Tremblay, B.; Manceron, L. *Chem. Phys*. **1999**, *242*, 235.

(23) Fournier, R. *J. Chem. Phys*. **1993**, *98*, 8041.

(24) Fournier, R. J. *Chem. Phys*. **1993**, *99*, 1801.

(25) Bauschlicher, C. W. *J. Chem. Phys*. **1994**, *100*, 1215.

(26) Barone, V. *Chem. Phys. Lett*. **1995**, *233*, 129.

(27) Barone, V. *J. Phys. Chem*. **1995**, *99*, 11659.

(28) Adamo, C.; Lelj, F. *J. Chem. Phys*. **1995**, *103*, 10605.

(29) Barone, V.; Adamo, C. *J. Phys. Chem*. **1996**, *100*, 2094.

(30) The predicted binding energy is reduced to 7.3 kcal/mol if BSSE and zero point vibrational energy corrections (1.6 and 0.6 kcal/mol, respectively) are included in the calculations, which is reasonably close to the experimental value of 6 ± 1 kcal/mol (see ref 31).

(31) Blitz, M. A.; Mitchell, S. A.; Hackett, P. A. *J. Phys. Chem*. **1991**, *95*, 8719.

(32) Calaminici, P.; Köster, A. M.; Russo, N.; Salahub, D. R. *J. Chem. Phys*. **1996**, *105*, 9546.

(33) Fournier, R. *J. Chem. Phys*. **1995**, *102*, 5396.

(34) Becker, A.; Langel, W.; Maass, S.; Knoezinger, E. *J. Phys. Chem*. **1993**, *97*, 5525.

(35) *Infrared and Raman spectra of Inorganic and Coordination Compounds*; Nakamoto, K., Ed.; Wiley-Interscience: New York, 1997.

(36) Chaban, G.; Gordon, M. S. *J. Chem. Phys*. **1997**, *107*, 2160.

(37) Bauschlicher, C. W.; Langhoff, S. R.; Barnes, L. A. *Chem. Phys*. **1989**, *129*, 431.

(38) Merle-Mejean, T.; Bouchareb, S.; Tranquille, M. *J. Phys. Chem*. **1989**, *93*, 1197.

(39) Galan, F.; Fouassier, M.; Tranquille, M.; Mascetti, J.; Pápai, I. *J. Phys. Chem*. **1997**, *101*, 2626.